Reduced Interference Vertex-Frequency Distributions

Ljubiša Stanković, *Fellow, IEEE*, Ervin Sejdić, *Senior Member, IEEE*, and Miloš Daković, *Member, IEEE*

***Abstract*—Vertex-frequency analysis of graph signals is a challenging topic for research and applications. Counterparts of the short-time Fourier transform, the wavelet transform, and the Rihaczek distribution have recently been introduced to the graph-signal analysis. In this letter, we have extended the energy distributions to a general reduced interference distributions class. It can improve the vertex-frequency representation of a graph signal while preserving the marginal properties. This class is related to the spectrogram of graph signals as well. Efficiency of the proposed representations is illustrated in examples.**

***Index Terms*—Energy distributions, graph-signal processing, time–frequency analysis, vertex-frequency analysis.**

I. Introduction

GRAPH-SIGNAL processing has become an active research area in recent years, resulting in many advanced solutions in various applications. In many practical cases, the signal domain is not a set of equidistant instants in time or a set of points in two-dimensional (2-D) or 3-D space placed on a regular rectangular grid. The data-sensing domain is then related to other parameters of the considered system/network. For example, in many social or web-related networks the sensing points and their connectivity are related to specific objects and their links. In some physical processes, other properties than the space or time coordinates define the relation between points where the signal is sensed. Even for the data sensed in the well-defined time and space domains, the introduction of relations between the sensing points in a form of graph may produce new insights and more advanced data-processing methods [1]–[5].

Spectral characteristics of graph signals can be vertex-varying. This corresponds to the time-varying signals and time–frequency analysis in classical signal processing [6]–[10]. Linear vertex-frequency analysis is introduced using strong correspondence with the short-time Fourier transform and the wavelet transform [11]–[15]. A different line of work has generalized the notion of time stationarity to signals defined on graphs [16], [17], developing windowing and energy spectral estimation schemes for graph-stationary signals [17]. In general, the classical time–frequency representations have many important properties whose extension to the graphs is not guaranteed, for example, the uncertainty principle.

Manuscript received April 23, 2018; revised July 18, 2018; accepted July 18, 2018. Date of publication; date of current version. The associate editor coordinating the review of this manuscript and approving it for publication was Dr. James E. Fowler. *(Corresponding author: Ljubiša Stanković.)*

L. Stanković and M. Daković are with the University of Montenegro, Podgorica 81000, Montenegro (e-mail: ljubisa@ac.me; milos@ac.me).

E. Sejdić is with the University of Pittsburgh, Pittsburg, PA 15213 USA (e-mail: esejdic@pitt.edu).

Color versions of one or more of the figures in this letter are available online at http://ieeexplore.ieee.org.

Digital Object Identifier 10.1109/LSP.2018.2860250

Recently, we have introduced a window-independent vertex-frequency energy distribution [24] based on the idea of the Rihaczek distribution [6], [9]. In this letter, the proposed distribution is extended to a class of vertex-frequency energy distributions satisfying marginal properties that are of high importance in the classical time–frequency analysis. These distributions are well localized in the vertex-frequency domain. They reduce interferences among components and provide a novel way for a systematic introduction of vertex-frequency energy distributions. The presented class provides a new insight into nonstationary graph-signal analysis. It can be used in the analysis of graph signals, for example, the EEG signals [5].

II. Vertex-Frequency Representations

A short review of the existing vertex-frequency representations will be presented here after basic definitions.

Consider a weighted graph with N vertices connected with edges. The weight of an edge that connects a vertex n with a vertex m is w_{nm}. If the vertices n and m are not connected then $w_{nm} = 0$. Edge weights are represented in a matrix form as a weight matrix $\mathbf{W}$, whose elements are w_{nm}. The diagonal elements of matrix $\mathbf{W}$ are zeros.

Signal $x(n)$, defined at each graph vertex n, is called graph signal. Signal samples $x(n)$ can be arranged in an $N \times 1$ column vector $\mathbf{x} = [x(1), x(2), \ldots, x(N)]^T$.

For undirected graphs, the weighting matrix $\mathbf{W}$ is symmetric, i.e., $w_{nm} = w_{mn}$. For these graphs, the Laplacian is defined as $\mathbf{L} = \mathbf{D} - \mathbf{W}$, where $\mathbf{D}$ is a diagonal matrix with $d_{nn} = \sum_{m=1}^{N} w_{nm}$ on the main diagonal. The eigenvalue decomposition of the Laplacian matrix reads as $\mathbf{L} = \mathbf{U}\mathbf{\Lambda}\mathbf{U}^T$, where $\mathbf{U}$ is a matrix of eigenvectors $\mathbf{u}_k$, $k = 1, 2, \ldots, N$ as its columns and $\mathbf{\Lambda}$ is a diagonal matrix with eigenvalues λ_k on the main diagonal. Here, we will assume that the eigenvalues are of the multiplicity one.

For an undirected graph, the spectrum of a graph signal (the graph discrete Fourier transform GDFT) is defined as $\mathbf{X} = \mathrm{GDFT}\{\mathbf{x}\} = \mathbf{U}^T\mathbf{x}$, where the vector $\mathbf{X}$ contains spectral coefficients $X(k)$ associated to the kth eigenvalue and the corresponding eigenvector

$$X(k) = \mathbf{u}_k^T\mathbf{x} = \sum_{n=1}^{N} x(n)u_k(n). \tag{1}$$

The inverse transformation is obtained as $\mathbf{x} = \mathbf{U}\mathbf{X}$, with

$$x(n) = \sum_{k=1}^{N} X(k)u_k(n). \tag{2}$$

Approaches that extend GDFT to directed graphs and graphs with repeated eigenvalues are proposed recently [18]–[20]. The eigen decomposition of the adjacency matrix $\mathbf{A}$ is commonly used for the directed graphs .

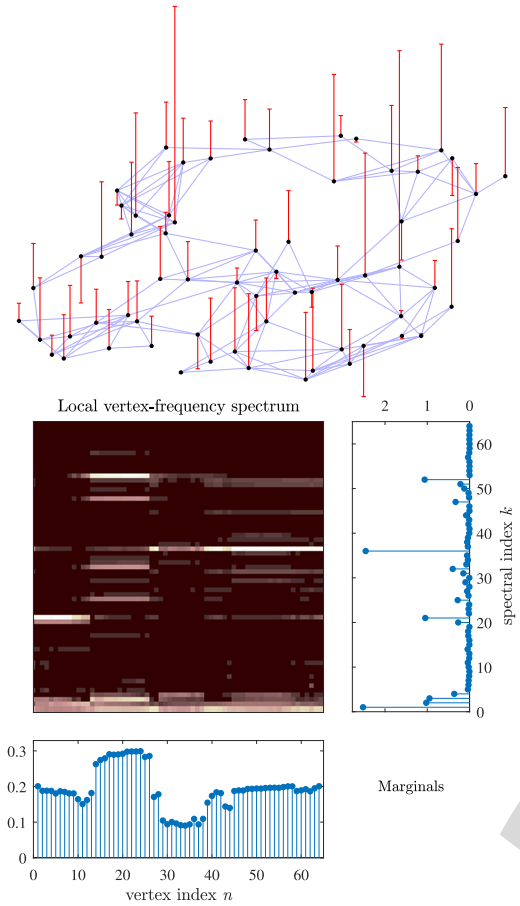

Fig. 1. Graph and a signal (top). Vertex-frequency representation using the spectrogram of graph signal (bottom). Marginal values are presented for the spectrogam, below and right.

A. Localized Vertex-Frequency Transforms

The localized vertex spectrum on a graph is an extension of the localized time (short time) Fourier transform [11]. It can be calculated as the spectrum of a signal $x(n)$ multiplied by a localization window function $h_n(m)$

$$S(n,k) = \sum_{m=1}^{N} x(m) h_n(m)\, u_k(m). \tag{3}$$

The window function $h_n(m)$ localizes the signal $x(m)$ around a vertex n. It can be defined using the vertex neighborhood [21] as $h_n(m) = g(d_{mn})$, where $g(d)$ corresponds to the basic window function in classical signal processing and d_{mn} is equal to the length of the shortest walk (distance) from the vertex m to the vertex n. The window $h_n(m)$ can also be defined using its spectral domain function $H(k)$

$$h_n(m) = \sum_{p=1}^{N} H(p) u_p(m) u_p(n) \tag{4}$$

where the spectral domain form is, for example, $H(k) = C\exp(-\lambda_k \tau)$, where C is the amplitude and $\tau > 0$ is a parameter that determines the window width [11].

A graph and a signal on this graph that will be used for illustrations are presented in Fig. 1(top). The graph signal is defined as a sum of: 1) constant component $u_0(n)$, 2) two

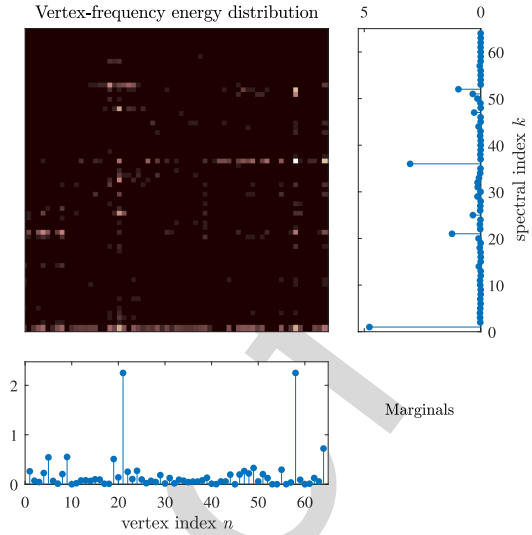

Fig. 2. Vertex-frequency energy distribution with its marginal values equal to $|x(n)|^2$ and $|X(k)|^2$, respectively.

delta pulses at vertices $n = 21$ and $n = 58$, and 3) parts of three eigenvectors $u_{20}(n)$, $u_{52}(n)$, and $u_{36}(n)$ over the vertex ranges $1 \le n \le 13$, $14 \le n \le 27$, $28 \le n \le N = 64$, respectively, with different weighing factors. This signal is analyzed using the vertex-frequency representation. For the parameter τ optimization, we have used the norm-one concentration measure, as in [10]. The optimal vertex-frequency representation, in a form of spectrogram $|S(n,k)|^2$, is presented in Fig. 1. We can see spread parts of components $u_k(n)$. The pulses are lost. The vertex and the spectral marginal properties are not satisfied. The values satisfying marginal properties are shown in Fig. 2.

For the optimization process with respect to τ, the vertex spectrogram should be normalized. One way to normalize the spectrogram is to divide the obtained norm-one with the norm-two of the spectrogram. The same result will be obtained if the localization windows are defined in such a way that the vertex spectrogram is energy unbiased

$$\sum_{n=1}^{N}\sum_{k=1}^{N} |S(n,k)|^2 = \sum_{n=1}^{N} |x(n)|^2 = E_x. \tag{5}$$

This condition is satisfied if

$$\sum_{n=1}^{N} |h_n(m)|^2 = 1 \tag{6}$$

for all m, since

$$\sum_{n=1}^{N}\sum_{k=1}^{N} |S(n,k)|^2 = \sum_{n=1}^{N}\sum_{m=1}^{N} |x(m)|^2 |h_n(m)|^2. \tag{7}$$

Optimization of parameter τ can be done by using more advanced techniques [22], [23] based on the graph-uncertainty principle. It is important to note that for any τ the vertex and frequency marginals cannot be simultaneously satisfied.

B. Vertex-Frequency Energy Distributions

Graph-signal energy (5), can be written as

$$E_x = \sum_{n=1}^{N} |x(n)|^2 = \sum_{n=1}^{N} x(n) \sum_{k=1}^{N} X^*(k) u_k^*(n).$$

or

$$E_x = \sum_{n=1}^{N} \sum_{k=1}^{N} x(n) X^*(k) u_k^*(n) = \sum_{n=1}^{N} \sum_{k=1}^{N} E(n,k)$$

where the energy vertex-frequency distribution is

$$E(n,k) = x(n) X^*(k) u_k^*(n). \tag{8}$$

This distribution corresponds to the Rihaczek distribution in time–frequency analysis. The vertex and frequency marginal properties of this distribution are

$$\sum_{n=1}^{N} E(n,k) = |X(k)|^2 \quad \text{and} \quad \sum_{k=1}^{N} E(n,k) = |x(n)|^2.$$

This energy distribution, along with the marginal properties, is illustrated in Fig. 2. The marginals are equal to $|x(n)|^2$ and $|X(k)|^2$ up to computer precision. We can see that the amplitude of component $u_0(n)$ is not constant and the pulses are not represented with vertical lines. This is due to strong interferences among components. To solve this problem in classical signal analysis the reduced interference distributions are introduced.

III. Reduced Interference Vertex-Frequency Energy Distributions

The general class of energy time–frequency distributions is extended to graph signals in this section. After a review of the classical Cohen class of distribution, conditions for the vertex-frequency marginal properties are derived. Few examples of the vertex-frequency energy distributions are given.

A. Review of the Classical Cohen Class of Distributions

Although it is known that any distribution can be used as the basis for the Cohen class of distribution, the Wigner distribution is commonly used [6], [8], [9]. Having in mind that the Wigner distribution is not suitable

for the graph-framework extension, here we will use the Rihaczek distribution as the basis. Since this kind of the Cohen class of distributions is not presented in common literature on time–frequency analysis, a short review of the Cohen class of distributions is presented. The Rihaczek distribution is $R(t,\omega) = x(t)X^*(\omega)\exp(-j\omega t)$ [6], [8], [9]. Its ambiguity domain form (a 2-D Fourier transform of $R(t,\omega)$ over t and ω) is $A(\theta,\tau) = \frac{1}{2\pi}\int_u X(u)X^*(u-\theta)\exp(j(u-\theta)\tau)du$.

The Cohen class of distributions, with the Rihaczek distribution as the basic distribution, is defined by $C(t,\omega) = \frac{1}{2\pi}\int_\theta \int_\tau A(\theta,\tau)c(\theta,\tau)\exp(-j\omega\tau)\exp(j\theta t)d\tau d\theta$, where $c(\theta,\tau)$ is the kernel function. Using the defined ambiguity domain form of the Rihaczek distribution $A(\theta,\tau)$ we get

$$C(t,\omega) = \frac{1}{4\pi^2}\int_u\int_v X(u)X^*(v)e^{jut}e^{-jvt} \times \int_\tau c(u-v,\tau)e^{-j\tau\omega}e^{j\tau u}d\tau du dv. \tag{9}$$

The frequency–frequency domain form of the Cohen class of distributions, with the Rihaczek distribution as the basis, is

$$C(t,\omega) = \int_u\int_v X(u)X^*(v)e^{jut}e^{-jvt}\phi(u-v,\omega-u)\frac{du dv}{4\pi^2}$$

where $\phi(u-v,\omega-u) = \int_\tau c(u-v,\tau)e^{-j\tau\omega}e^{j\tau u}d\tau$.

The marginal properties are met if the kernel $c(\theta,\tau)$ satisfies the conditions $c(\theta,0)=1$ and $c(0,\tau)=1$.

B. Reduced Interference Distributions on Graphs

We will first consider the frequency–frequency domain of the general energy distributions satisfying the marginal properties. The frequency-domain definition of the presented energy distribution (8) is

$$E(n,k) = x(n)X^*(k)u_k^*(n) = \sum_{p=1}^{N} X(p)X^*(k)u_p(n)u_k^*(n).$$

Therefore, the general graph-distribution form is

$$G(n,k) = \sum_{p=1}^{N}\sum_{q=1}^{N} X(p)X^*(q)u_p(n)u_q^*(n)\phi(p,k,q). \tag{10}$$

For $\phi(p,k,q) = \delta(q-k)$ the graph Rihaczek distribution (8) follows. The unbiased energy condition $\sum_{k=1}^{N}\sum_{n=1}^{N} G(n,k) = E_x$ is satisfied if

$$\sum_{k=1}^{N}\phi(p,k,p) = 1.$$

The distribution $G(n,k)$ may satisfy the vertex and frequency marginal properties given as next.

1) The vertex marginal property is satisfied if

$$\sum_{k=1}^{N}\phi(p,k,q) = 1$$

since

$$\sum_{k=1}^{N} G(n,k) = \sum_{p=1}^{N}\sum_{q=1}^{N} X(p)X^*(q)u_p(n)u_q^*(n) = |x(n)|^2.$$

The same condition is required for the vertex moment property $\sum_{n=1}^{N}\sum_{k=1}^{N} n^m G(n,k) = \sum_{n=1}^{N} n^m |x(n)|^2$.

2) The frequency marginal property is satisfied if

$$\phi(p,k,p) = \delta(p-k).$$

Then, the sum over vertex index produces

$$\sum_{n=1}^{N} G(n,k) = \sum_{p=1}^{N} |X(p)|^2\phi(p,k,p) = |X(k)|^2$$

since $\sum_{n=1}^{N} u_p(n)u_q^*(n) = \delta(p-q)$, i.e., the eigenvectors are orthonormal. If the frequency marginal property holds, then the frequency moment property holds as well, $\sum_{n=1}^{N}\sum_{k=1}^{N} k^m G(n,k) = \sum_{k=1}^{N} k^m |X(k)|^2$.

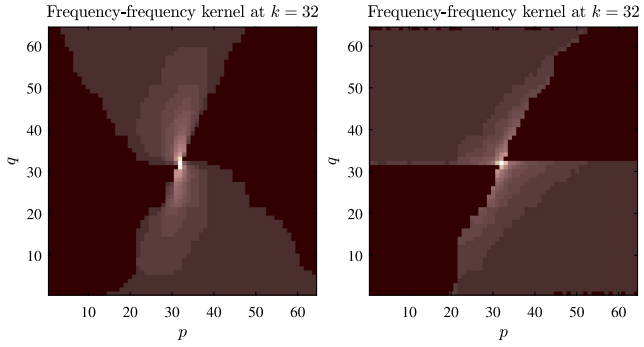

Fig. 3. Frequency–frequency domain kernels: The exponential kernel (left) and the Sinc kernel (right), at $k = N/2 = 32$.

C. Reduced Interference Distribution Kernels

A few examples of the reduced interference kernels that satisfy marginal properties will be presented next.

Choi–Williams kernel: The classic form of this kernel is $c(\theta,\tau) = \exp\left(-\theta^2\tau^2/(2\sigma^2)\right)$. The frequency–frequency form of this kernel is $\phi(\theta,\omega) = \mathrm{FT}_\tau\{c(\theta,\tau)\} = \exp\left(-\omega^2\sigma^2/(2\theta^2)\right)|\sigma/\theta|\sqrt{2\pi}$. Its shifted version would be

$$\phi(u-v,\omega-u) = \frac{\sigma\sqrt{2\pi}}{|v-u|}\exp\left(-\sigma^2\frac{(\omega-u)^2}{2(v-u)^2}\right).$$

A straightforward extension to the graph-signal processing would be to use the relation $\lambda \sim \omega^2$, with appropriate exponential kernel normalization. We have implemented this form and concluded that it produces results similar to the simplified form that satisfies the marginal properties and decays in the frequency–frequency domain. The form of this kernel is

$$\phi(p,k,q) = \frac{1}{s(q,p)}\exp\left(-\alpha\frac{|\lambda_p-\lambda_k|}{|\lambda_p-\lambda_q|}\right)$$

where $s(q,p) = \sum_{k=1}^{N}\exp\left(-\alpha\frac{|\lambda_p-\lambda_k|}{|\lambda_p-\lambda_q|}\right)$ for $q \neq p$ and $\phi(p,k,p) = \delta(k-p)$. It satisfies both marginal properties.

The vertex-frequency distribution with the exponential kernel [see Fig. 3(left)] is presented in Fig. 4. This kind of distribution presents correctly constant component $u_0(n)$, two delta pulses at vertices $n = 21$ and $n = 58$, and parts of other three eigenvectors, preserving the marginal properties.

Sinc kernel: The simplest reduced interference kernel in the frequency–frequency domain that would satisfy the marginal properties, is the Sinc kernel. Its form is

$$\phi(p,k,q) = \begin{cases} \dfrac{1}{1+2|p-q|} & \text{for } |k-p| \le |p-q| \\ 0 & \text{otherwise} \end{cases}$$

This kernel, with appropriate normalization, is shown in Fig. 3(right), for $k = 32$. A vertex-frequency representation with this kernel would be similar to the one shown in Fig. 4.

Separable kernels: If the kernel is separable, such that $\phi(p,k,q) = g(k-p)g(k-q)$, then we can write $G(n,k) = |\sum_{p=1}^{N} X(p)g(k-p)u_p(n)|^2$. This is a frequency-domain definition of the graph spectrogram. Relation between the vertex-domain spectrogram (3) and the frequency–frequency domain distribution is complex.

The separable kernels cannot satisfy the marginal properties since $\delta(k-p) = \phi(p,k,p) = g^2(k-p)$ means $g(k-p) = \delta(k-p)$. These kernels do not satisfy $\sum_{k=1}^{N}\phi(p,k,q) = 1$ for all p and q.

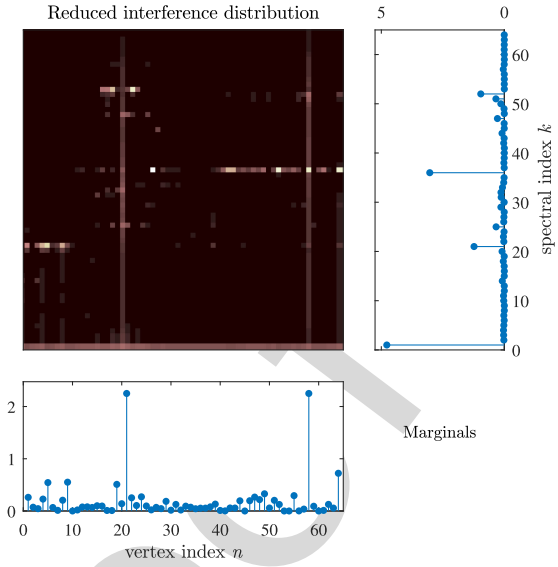

Fig. 4. Vertex-frequency reduced interference distribution using the kernel from Fig. 3(left) with its marginal values equal to $|x(n)|^2$ and $|X(k)|^2$, respectively.

Vertex–vertex shift domain distribution: The general vertex-frequency distribution can be written for the vertex–vertex shift domain as a dual form to (10)

$$G(n,k) = \sum_{m=1}^{N}\sum_{l=1}^{N} x(m)x^*(l)u_k(m)u_k^*(l)\varphi(m,n,l) \quad (11)$$

where $\varphi(m,n,l)$ is the kernel in this domain (the same mathematical form as the frequency–frequency domain kernel). The frequency marginal is satisfied if $\sum_{n=1}^{N}\varphi(m,n,l) = 1$ holds. The vertex marginal is met if $\varphi(m,n,m) = \delta(m-n)$. The relation of this distribution with the vertex domain spectrogram (3) is simple using

$$\varphi(m,n,l) = h_n(m)h_n^*(l)$$
$$= \sum_{p=1}^{N}\sum_{q=1}^{N} H(p)H^*(q)u_p(m)u_p(n)u_q^*(l)u_q^*(n).$$

This kernel is defined by the frequency-domain window form $H(p)$. It cannot satisfy both marginal properties. The unbiased energy condition $\sum_{n=1}^{N}\varphi(m,n,m) = 1$ reduces to (6).

Classical time–frequency analysis: The approach presented in this letter can be used for the directed graphs and adjacency matrices as well. The classical Fourier and time–frequency analysis follow from a directed ring graph. The adjacency matrix decomposition produces complex-valued eigenvectors of form $u_k(n) = \exp\left(j2\pi nk/N\right)/\sqrt{N}$.

IV. Conclusion

In this letter, reduced interference vertex-frequency distributions were introduced. The main advantage of these distributions is that they can produce a signal representation with high energy concentration while reducing interferences and preserving the vertex and frequency marginal property.

REFERENCES

[1] S. Chen, R. Varma, A. Sandryhaila, and J. Kovačević, "Discrete Signal Processing on Graphs: Sampling Theory," *IEEE Trans. Signal Process.*, vol. 63, no. 24, pp. 6510–6523, Dec. 2015.

[2] A. Sandryhaila and J. M. F. Moura, "Discrete signal processing on graphs," *IEEE. Trans. Signal Process.*, vol. 61, no. 7, pp. 1644–1656, Apr. 2013.

[3] A. Sandryhaila and J. M. F. Moura, "Discrete signal processing on graphs: Frequency analysis," *IEEE. Trans. Signal Process.*, vol. 62, no. 12, pp. 3042–3054, Jun. 2014.

[4] D. I. Shuman, S. K. Narang, P. Frossard, A. Ortega, and P. Vandergheynst, "The emerging field of signal processing on graphs: Extending high-dimensional data analysis to networks and other irregular domains," *IEEE Signal Process. Mag.*, vol. 30, no. 3, pp. 83–98, May 2013.

[5] I. Jestrović, J. L. Coyle, and E. Sejdić, "Differences in brain networks during consecutive swallows detected using an optimized vertex-frequency algorithm," *Neuroscience*, vol. 344, pp. 113–123, 2017.

[6] L. Stanković, M. Daković, and T. Thayaparan, *Time-Frequency Signal Analysis with Applications*, Norwood, MA, USA: Artech House, Mar. 2013.

[7] N. E. Huang *et al.*, "The empirical mode decomposition and the Hilbert spectrum for nonlinear and non-stationary time series analysis," *Proc. Roy. Soc. London A, Math., Phys. Eng. Sci.*, vol. 454, no. 1971, 1998.

[8] L. Cohen, *Time-frequency Analysis*. Upper Saddle River, NJ, USA: Prentice-Hall, 1995.

[9] B. Boashash, ed, *Time-Frequency Signal Analysis and Processing, A Comprehensive Reference*, New York, NY, USA: Academic, 2015.

[10] L. Stanković, "A measure of some time–frequency distributions concentration," *Signal Process.*, vol. 81, no. 3, pp. 621–631, Mar. 2001.

[11] D. I. Shuman, B. Ricaud, and P. Vandergheynst, "Vertex-frequency analysis on graphs," *Appl. Comput. Harmon. Anal.*, vol. 40, no. 2, pp. 260–291, Mar. 2016.

[12] H. Behjat, U. Richter, D. Van De Ville, and L. Sornmo, "Signal-adapted tight frames on graphs," *IEEE Trans. Signal Process.*, vol. 64, no. 22, pp. 6017–6029, Nov. 2016.

[13] D. Hammond, P. Vandergheynst, and R. Gribonval, "Wavelets on graphs via spectral graph theory," *Appl. Comput. Harmon. Anal.*, vol. 30, no. 2, pp. 129–150, 2011.

[14] A. Sakiyama and Y. Tanaka, "Oversampled graph Laplacian matrix for graph filter banks," *IEEE Trans. Signal Process.*, vol. 62, no. 24, pp. 6425–6437, Dec. 2014.

[15] I. Jestrović, J. L. Coyle, and E. Sejdić, "A fast algorithm for vertex-frequency representations of signals on graphs," *Signal Process.*, vol. 131, pp. 483–491, Feb. 2017.

[16] B. Girault, "Stationary graph signals using an isometric graph translation," in *Proc. Eur. Signal Process. Conf.*, 2015, pp. 1516–1520.

[17] A. G. Marques, S. Segarra, G. Leus, and A. Ribeiro, "Stationary graph processes and spectral estimation," *IEEE Trans. Signal Process.*, vol. 65, no. 22, pp. 5911–5926, Nov. 2017, doi: 10.1109/TSP.2017.2739099.

[18] S. Sardellitti, S. Barbarossa, and P. Di Lorenzo, "On the graph Fourier transform for directed graphs," *IEEE J. Sel. Topics Signal Process.*, vol. 11, no. 6, pp. 796–811, Sep. 2017.

[19] J. A. Deri and J. M. Moura, "Spectral projector-based graph Fourier transforms," *IEEE J. Sel. Topics Signal Process.*, vol. 11, no. 6, pp. 785–795, Sep. 2017.

[20] R. Shafipour, A. Khodabakhsh, G. Mateos, and E. Nikolova, "A digraph Fourier transform with spread frequency components," arXiv:1705.10821

[21] L. Stanković, M. Daković, and E. Sejdić, "Vertex-frequency analysis: A way to localize graph spectral components," *IEEE Signal Process. Mag.*, vol. 34, no. 4, pp. 176–182, Jul. 2017.

[22] M. Tsitsvero, S. Barbarossa, and P. Di Lorenzo, "Signals on graphs: Uncertainty principle and sampling," *IEEE Trans. Signal Process.*, vol. 64, no. 18, pp. 4845–4860, Sep. 2016.

[23] A. Agaskar and Y. M. Lu, "A spectral graph uncertainty principle," *IEEE Trans. Inf. Theory*, vol. 59, no. 7, pp. 4338–4356, Jul. 2013.

[24] L. Stanković, M. Daković, and E. Sejdić, "Vertex-frequency energy distributions," *IEEE Signal Process. Lett.*, vol. 25, no. 3, pp. 358–362, Mar. 2018.

GENERAL INSTRUCTION

- **Authors: We cannot accept new source files as corrections for your paper. If possible, please annotate the PDF proof we have sent you with your corrections and upload it via the Author Gateway. Alternatively, you may send us your corrections in list format. You may also upload revised graphics via the Author Gateway.**

QUERIES

Q1. Author: Please confirm or add details for any funding or financial support for the research of this article.
Q2. Author: Please check if the postal code in the affiliation for the author E. Sejdić is okay as set.
Q3. Author: Please provide the full form of acronym GDFT and define it on its first occurrence.
Q4. Author: Please provide the book's author's name for Ref. [9].
Q5. Author: Please update Ref. [20].

Reduced Interference Vertex-Frequency Distributions

Ljubiša Stanković, *Fellow, IEEE*, Ervin Sejdić, *Senior Member, IEEE*, and Miloš Daković, *Member, IEEE*

***Abstract*—Vertex-frequency analysis of graph signals is a challenging topic for research and applications. Counterparts of the short-time Fourier transform, the wavelet transform, and the Rihaczek distribution have recently been introduced to the graph-signal analysis. In this letter, we have extended the energy distributions to a general reduced interference distributions class. It can improve the vertex-frequency representation of a graph signal while preserving the marginal properties. This class is related to the spectrogram of graph signals as well. Efficiency of the proposed representations is illustrated in examples.**

***Index Terms*—Energy distributions, graph-signal processing, time–frequency analysis, vertex-frequency analysis.**

I. Introduction

GRAPH-SIGNAL processing has become an active research area in recent years, resulting in many advanced solutions in various applications. In many practical cases, the signal domain is not a set of equidistant instants in time or a set of points in two-dimensional (2-D) or 3-D space placed on a regular rectangular grid. The data-sensing domain is then related to other parameters of the considered system/network. For example, in many social or web-related networks the sensing points and their connectivity are related to specific objects and their links. In some physical processes, other properties than the space or time coordinates define the relation between points where the signal is sensed. Even for the data sensed in the well-defined time and space domains, the introduction of relations between the sensing points in a form of graph may produce new insights and more advanced data-processing methods [1]–[5].

Spectral characteristics of graph signals can be vertex-varying. This corresponds to the time-varying signals and time–frequency analysis in classical signal processing [6]–[10]. Linear vertex-frequency analysis is introduced using strong correspondence with the short-time Fourier transform and the wavelet transform [11]–[15]. A different line of work has generalized the notion of time stationarity to signals defined on graphs [16], [17], developing windowing and energy spectral estimation schemes for graph-stationary signals [17]. In general, the classical time–frequency representations have many important properties whose extension to the graphs is not guaranteed, for example, the uncertainty principle.

Manuscript received April 23, 2018; revised July 18, 2018; accepted July 18, 2018. Date of publication; date of current version. The associate editor coordinating the review of this manuscript and approving it for publication was Dr. James E. Fowler. *(Corresponding author: Ljubiša Stanković.)*

L. Stanković and M. Daković are with the University of Montenegro, Podgorica 81000, Montenegro (e-mail: ljubisa@ac.me; milos@ac.me).

E. Sejdić is with the University of Pittsburgh, Pittsburg, PA 15213 USA (e-mail: esejdic@pitt.edu).

Color versions of one or more of the figures in this letter are available online at http://ieeexplore.ieee.org.

Digital Object Identifier 10.1109/LSP.2018.2860250

Recently, we have introduced a window-independent vertex-frequency energy distribution [24] based on the idea of the Rihaczek distribution [6], [9]. In this letter, the proposed distribution is extended to a class of vertex-frequency energy distributions satisfying marginal properties that are of high importance in the classical time–frequency analysis. These distributions are well localized in the vertex-frequency domain. They reduce interferences among components and provide a novel way for a systematic introduction of vertex-frequency energy distributions. The presented class provides a new insight into nonstationary graph-signal analysis. It can be used in the analysis of graph signals, for example, the EEG signals [5].

II. Vertex-Frequency Representations

A short review of the existing vertex-frequency representations will be presented here after basic definitions.

Consider a weighted graph with N vertices connected with edges. The weight of an edge that connects a vertex n with a vertex m is w_{nm}. If the vertices n and m are not connected then $w_{nm} = 0$. Edge weights are represented in a matrix form as a weight matrix $\mathbf{W}$, whose elements are w_{nm}. The diagonal elements of matrix $\mathbf{W}$ are zeros.

Signal $x(n)$, defined at each graph vertex n, is called graph signal. Signal samples $x(n)$ can be arranged in an $N \times 1$ column vector $\mathbf{x} = [x(1), x(2), \ldots, x(N)]^T$.

For undirected graphs, the weighting matrix $\mathbf{W}$ is symmetric, i.e., $w_{nm} = w_{mn}$. For these graphs, the Laplacian is defined as $\mathbf{L} = \mathbf{D} - \mathbf{W}$, where $\mathbf{D}$ is a diagonal matrix with $d_{nn} = \sum_{m=1}^{N} w_{nm}$ on the main diagonal. The eigenvalue decomposition of the Laplacian matrix reads as $\mathbf{L} = \mathbf{U}\mathbf{\Lambda}\mathbf{U}^T$, where $\mathbf{U}$ is a matrix of eigenvectors $\mathbf{u}_k$, $k = 1, 2, \ldots, N$ as its columns and $\mathbf{\Lambda}$ is a diagonal matrix with eigenvalues λ_k on the main diagonal. Here, we will assume that the eigenvalues are of the multiplicity one.

For an undirected graph, the spectrum of a graph signal (the graph discrete Fourier transform GDFT) is defined as $\mathbf{X} = \mathrm{GDFT}\{\mathbf{x}\} = \mathbf{U}^T\mathbf{x}$, where the vector $\mathbf{X}$ contains spectral coefficients $X(k)$ associated to the kth eigenvalue and the corresponding eigenvector

$$X(k) = \mathbf{u}_k^T\mathbf{x} = \sum_{n=1}^{N} x(n)u_k(n). \tag{1}$$

The inverse transformation is obtained as $\mathbf{x} = \mathbf{U}\mathbf{X}$, with

$$x(n) = \sum_{k=1}^{N} X(k)u_k(n). \tag{2}$$

Approaches that extend GDFT to directed graphs and graphs with repeated eigenvalues are proposed recently [18]–[20]. The eigen decomposition of the adjacency matrix $\mathbf{A}$ is commonly used for the directed graphs .

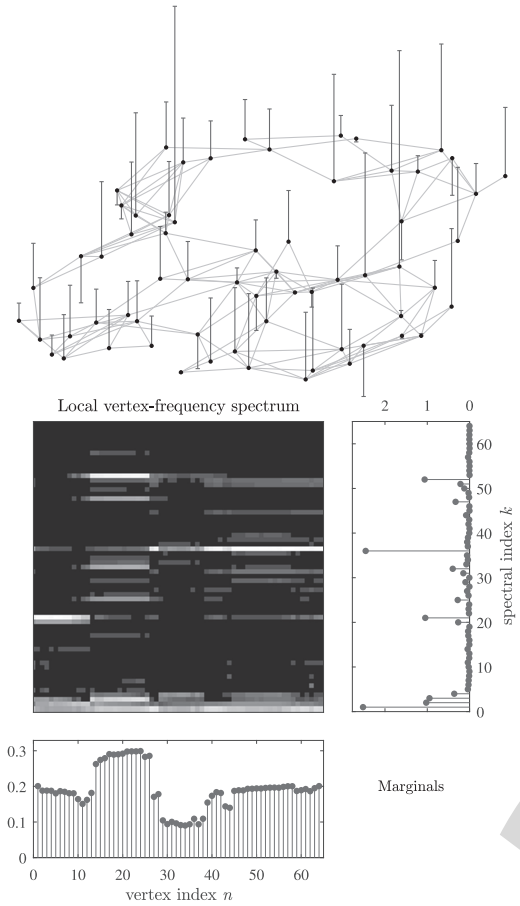

Fig. 1. Graph and a signal (top). Vertex-frequency representation using the spectrogram of graph signal (bottom). Marginal values are presented for the spectrogam, below and right.

A. Localized Vertex-Frequency Transforms

The localized vertex spectrum on a graph is an extension of the localized time (short time) Fourier transform [11]. It can be calculated as the spectrum of a signal $x(n)$ multiplied by a localization window function $h_n(m)$

$$S(n,k) = \sum_{m=1}^{N} x(m) h_n(m)\, u_k(m). \tag{3}$$

The window function $h_n(m)$ localizes the signal $x(m)$ around a vertex n. It can be defined using the vertex neighborhood [21] as $h_n(m) = g(d_{mn})$, where $g(d)$ corresponds to the basic window function in classical signal processing and d_{mn} is equal to the length of the shortest walk (distance) from the vertex m to the vertex n. The window $h_n(m)$ can also be defined using its spectral domain function $H(k)$

$$h_n(m) = \sum_{p=1}^{N} H(p) u_p(m) u_p(n) \tag{4}$$

where the spectral domain form is, for example, $H(k) = C\exp(-\lambda_k \tau)$, where C is the amplitude and $\tau > 0$ is a parameter that determines the window width [11].

A graph and a signal on this graph that will be used for illustrations are presented in Fig. 1(top). The graph signal is defined as a sum of: 1) constant component $u_0(n)$, 2) two

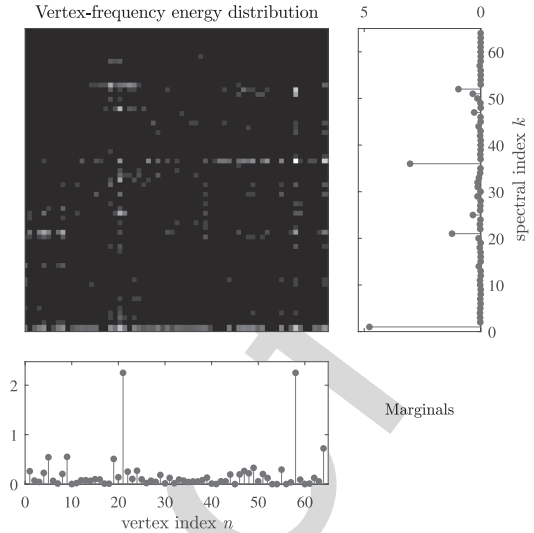

Fig. 2. Vertex-frequency energy distribution with its marginal values equal to $|x(n)|^2$ and $|X(k)|^2$, respectively.

delta pulses at vertices $n = 21$ and $n = 58$, and 3) parts of three eigenvectors $u_{20}(n)$, $u_{52}(n)$, and $u_{36}(n)$ over the vertex ranges $1 \le n \le 13$, $14 \le n \le 27$, $28 \le n \le N = 64$, respectively, with different weighing factors. This signal is analyzed using the vertex-frequency representation. For the parameter τ optimization, we have used the norm-one concentration measure, as in [10]. The optimal vertex-frequency representation, in a form of spectrogram $|S(n,k)|^2$, is presented in Fig. 1. We can see spread parts of components $u_k(n)$. The pulses are lost. The vertex and the spectral marginal properties are not satisfied. The values satisfying marginal properties are shown in Fig. 2.

For the optimization process with respect to τ, the vertex spectrogram should be normalized. One way to normalize the spectrogram is to divide the obtained norm-one with the norm-two of the spectrogram. The same result will be obtained if the localization windows are defined in such a way that the vertex spectrogram is energy unbiased

$$\sum_{n=1}^{N}\sum_{k=1}^{N} |S(n,k)|^2 = \sum_{n=1}^{N} |x(n)|^2 = E_x. \tag{5}$$

This condition is satisfied if

$$\sum_{n=1}^{N} |h_n(m)|^2 = 1 \tag{6}$$

for all m, since

$$\sum_{n=1}^{N}\sum_{k=1}^{N} |S(n,k)|^2 = \sum_{n=1}^{N}\sum_{m=1}^{N} |x(m)|^2 |h_n(m)|^2. \tag{7}$$

Optimization of parameter τ can be done by using more advanced techniques [22], [23] based on the graph-uncertainty principle. It is important to note that for any τ the vertex and frequency marginals cannot be simultaneously satisfied.

B. Vertex-Frequency Energy Distributions

Graph-signal energy (5), can be written as

$$E_x = \sum_{n=1}^{N} |x(n)|^2 = \sum_{n=1}^{N} x(n) \sum_{k=1}^{N} X^*(k) u_k^*(n).$$

or

$$E_x = \sum_{n=1}^{N} \sum_{k=1}^{N} x(n) X^*(k) u_k^*(n) = \sum_{n=1}^{N} \sum_{k=1}^{N} E(n,k)$$

where the energy vertex-frequency distribution is

$$E(n,k) = x(n) X^*(k) u_k^*(n). \tag{8}$$

This distribution corresponds to the Rihaczek distribution in time–frequency analysis. The vertex and frequency marginal properties of this distribution are

$$\sum_{n=1}^{N} E(n,k) = |X(k)|^2 \quad \text{and} \quad \sum_{k=1}^{N} E(n,k) = |x(n)|^2.$$

This energy distribution, along with the marginal properties, is illustrated in Fig. 2. The marginals are equal to $|x(n)|^2$ and $|X(k)|^2$ up to computer precision. We can see that the amplitude of component $u_0(n)$ is not constant and the pulses are not represented with vertical lines. This is due to strong interferences among components. To solve this problem in classical signal analysis the reduced interference distributions are introduced.

III. Reduced Interference Vertex-Frequency Energy Distributions

The general class of energy time–frequency distributions is extended to graph signals in this section. After a review of the classical Cohen class of distribution, conditions for the vertex-frequency marginal properties are derived. Few examples of the vertex-frequency energy distributions are given.

A. Review of the Classical Cohen Class of Distributions

Although it is known that any distribution can be used as the basis for the Cohen class of distribution, the Wigner distribution is commonly used [6], [8], [9]. Having in mind that the Wigner distribution is not suitable

for the graph-framework extension, here we will use the Rihaczek distribution as the basis. Since this kind of the Cohen class of distributions is not presented in common literature on time–frequency analysis, a short review of the Cohen class of distributions is presented. The Rihaczek distribution is $R(t,\omega) = x(t)X^*(\omega)\exp(-j\omega t)$ [6], [8], [9]. Its ambiguity domain form (a 2-D Fourier transform of $R(t,\omega)$ over t and ω) is $A(\theta,\tau) = \frac{1}{2\pi}\int_u X(u)X^*(u-\theta)\exp(j(u-\theta)\tau)du$.

The Cohen class of distributions, with the Rihaczek distribution as the basic distribution, is defined by $C(t,\omega) = \frac{1}{2\pi}\int_\theta \int_\tau A(\theta,\tau)c(\theta,\tau)\exp(-j\omega\tau)\exp(j\theta t)d\tau d\theta$, where $c(\theta,\tau)$ is the kernel function. Using the defined ambiguity domain form of the Rihaczek distribution $A(\theta,\tau)$ we get

$$C(t,\omega) = \frac{1}{4\pi^2}\int_u\int_v X(u)X^*(v)e^{jut}e^{-jvt} \times \int_\tau c(u-v,\tau)e^{-j\tau\omega}e^{j\tau u}d\tau du dv. \tag{9}$$

The frequency–frequency domain form of the Cohen class of distributions, with the Rihaczek distribution as the basis, is

$$C(t,\omega) = \int_u\int_v X(u)X^*(v)e^{jut}e^{-jvt}\phi(u-v,\omega-u)\frac{du dv}{4\pi^2}$$

where $\phi(u-v,\omega-u) = \int_\tau c(u-v,\tau)e^{-j\tau\omega}e^{j\tau u}d\tau$.

The marginal properties are met if the kernel $c(\theta,\tau)$ satisfies the conditions $c(\theta,0)=1$ and $c(0,\tau)=1$.

B. Reduced Interference Distributions on Graphs

We will first consider the frequency–frequency domain of the general energy distributions satisfying the marginal properties. The frequency-domain definition of the presented energy distribution (8) is

$$E(n,k) = x(n)X^*(k)u_k^*(n) = \sum_{p=1}^{N} X(p)X^*(k)u_p(n)u_k^*(n).$$

Therefore, the general graph-distribution form is

$$G(n,k) = \sum_{p=1}^{N}\sum_{q=1}^{N} X(p)X^*(q)u_p(n)u_q^*(n)\phi(p,k,q). \tag{10}$$

For $\phi(p,k,q) = \delta(q-k)$ the graph Rihaczek distribution (8) follows. The unbiased energy condition $\sum_{k=1}^{N}\sum_{n=1}^{N} G(n,k) = E_x$ is satisfied if

$$\sum_{k=1}^{N}\phi(p,k,p) = 1.$$

The distribution $G(n,k)$ may satisfy the vertex and frequency marginal properties given as next.

1) The vertex marginal property is satisfied if

$$\sum_{k=1}^{N}\phi(p,k,q) = 1$$

since

$$\sum_{k=1}^{N} G(n,k) = \sum_{p=1}^{N}\sum_{q=1}^{N} X(p)X^*(q)u_p(n)u_q^*(n) = |x(n)|^2.$$

The same condition is required for the vertex moment property $\sum_{n=1}^{N}\sum_{k=1}^{N} n^m G(n,k) = \sum_{n=1}^{N} n^m |x(n)|^2$.

2) The frequency marginal property is satisfied if

$$\phi(p,k,p) = \delta(p-k).$$

Then, the sum over vertex index produces

$$\sum_{n=1}^{N} G(n,k) = \sum_{p=1}^{N} |X(p)|^2\phi(p,k,p) = |X(k)|^2$$

since $\sum_{n=1}^{N} u_p(n)u_q^*(n) = \delta(p-q)$, i.e., the eigenvectors are orthonormal. If the frequency marginal property holds, then the frequency moment property holds as well, $\sum_{n=1}^{N}\sum_{k=1}^{N} k^m G(n,k) = \sum_{k=1}^{N} k^m |X(k)|^2$.

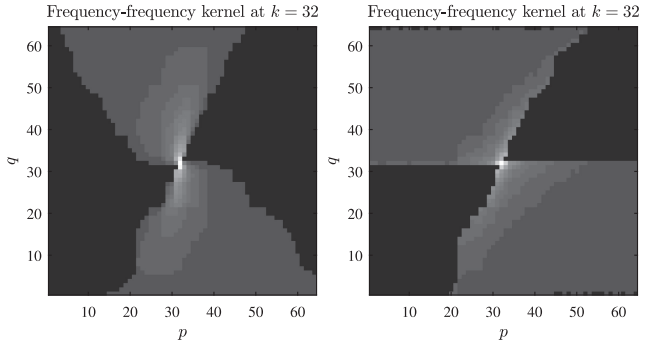

Fig. 3. Frequency–frequency domain kernels: The exponential kernel (left) and the Sinc kernel (right), at $k = N/2 = 32$.

C. Reduced Interference Distribution Kernels

A few examples of the reduced interference kernels that satisfy marginal properties will be presented next.

Choi–Williams kernel: The classic form of this kernel is $c(\theta,\tau) = \exp\left(-\theta^2\tau^2/(2\sigma^2)\right)$. The frequency–frequency form of this kernel is $\phi(\theta,\omega) = \mathrm{FT}_\tau\{c(\theta,\tau)\} = \exp\left(-\omega^2\sigma^2/(2\theta^2)\right)|\sigma/\theta|\sqrt{2\pi}$. Its shifted version would be

$$\phi(u-v,\omega-u) = \frac{\sigma\sqrt{2\pi}}{|v-u|}\exp\left(-\sigma^2\frac{(\omega-u)^2}{2(v-u)^2}\right).$$

A straightforward extension to the graph-signal processing would be to use the relation $\lambda \sim \omega^2$, with appropriate exponential kernel normalization. We have implemented this form and concluded that it produces results similar to the simplified form that satisfies the marginal properties and decays in the frequency–frequency domain. The form of this kernel is

$$\phi(p,k,q) = \frac{1}{s(q,p)}\exp\left(-\alpha\frac{|\lambda_p-\lambda_k|}{|\lambda_p-\lambda_q|}\right)$$

where $s(q,p) = \sum_{k=1}^{N}\exp\left(-\alpha\frac{|\lambda_p-\lambda_k|}{|\lambda_p-\lambda_q|}\right)$ for $q \neq p$ and $\phi(p,k,p) = \delta(k-p)$. It satisfies both marginal properties.

The vertex-frequency distribution with the exponential kernel [see Fig. 3(left)] is presented in Fig. 4. This kind of distribution presents correctly constant component $u_0(n)$, two delta pulses at vertices $n = 21$ and $n = 58$, and parts of other three eigenvectors, preserving the marginal properties.

Sinc kernel: The simplest reduced interference kernel in the frequency–frequency domain that would satisfy the marginal properties, is the Sinc kernel. Its form is

$$\phi(p,k,q) = \begin{cases} \dfrac{1}{1+2|p-q|} & \text{for } |k-p| \le |p-q| \\ 0 & \text{otherwise} \end{cases}$$

This kernel, with appropriate normalization, is shown in Fig. 3(right), for $k = 32$. A vertex-frequency representation with this kernel would be similar to the one shown in Fig. 4.

Separable kernels: If the kernel is separable, such that $\phi(p,k,q) = g(k-p)g(k-q)$, then we can write $G(n,k) = |\sum_{p=1}^{N} X(p)g(k-p)u_p(n)|^2$. This is a frequency-domain definition of the graph spectrogram. Relation between the vertex-domain spectrogram (3) and the frequency–frequency domain distribution is complex.

The separable kernels cannot satisfy the marginal properties since $\delta(k-p) = \phi(p,k,p) = g^2(k-p)$ means $g(k-p) = \delta(k-p)$. These kernels do not satisfy $\sum_{k=1}^{N}\phi(p,k,q) = 1$ for all p and q.

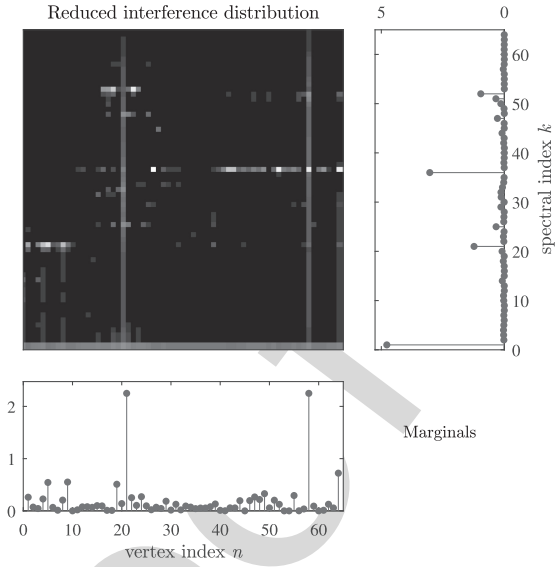

Fig. 4. Vertex-frequency reduced interference distribution using the kernel from Fig. 3(left) with its marginal values equal to $|x(n)|^2$ and $|X(k)|^2$, respectively.

Vertex–vertex shift domain distribution: The general vertex-frequency distribution can be written for the vertex–vertex shift domain as a dual form to (10)

$$G(n,k) = \sum_{m=1}^{N}\sum_{l=1}^{N} x(m)x^*(l)u_k(m)u_k^*(l)\varphi(m,n,l) \quad (11)$$

where $\varphi(m,n,l)$ is the kernel in this domain (the same mathematical form as the frequency–frequency domain kernel). The frequency marginal is satisfied if $\sum_{n=1}^{N}\varphi(m,n,l) = 1$ holds. The vertex marginal is met if $\varphi(m,n,m) = \delta(m-n)$. The relation of this distribution with the vertex domain spectrogram (3) is simple using

$$\begin{aligned}\varphi(m,n,l) &= h_n(m)h_n^*(l) \\ &= \sum_{p=1}^{N}\sum_{q=1}^{N} H(p)H^*(q)u_p(m)u_p(n)u_q^*(l)u_q^*(n).\end{aligned}$$

This kernel is defined by the frequency-domain window form $H(p)$. It cannot satisfy both marginal properties. The unbiased energy condition $\sum_{n=1}^{N}\varphi(m,n,m) = 1$ reduces to (6).

Classical time–frequency analysis: The approach presented in this letter can be used for the directed graphs and adjacency matrices as well. The classical Fourier and time–frequency analysis follow from a directed ring graph. The adjacency matrix decomposition produces complex-valued eigenvectors of form $u_k(n) = \exp(j2\pi nk/N)/\sqrt{N}$.

IV. Conclusion

In this letter, reduced interference vertex-frequency distributions were introduced. The main advantage of these distributions is that they can produce a signal representation with high energy concentration while reducing interferences and preserving the vertex and frequency marginal property.

REFERENCES

[1] S. Chen, R. Varma, A. Sandryhaila, and J. Kovačević, "Discrete Signal Processing on Graphs: Sampling Theory," *IEEE Trans. Signal Process.*, vol. 63, no. 24, pp. 6510–6523, Dec. 2015.

[2] A. Sandryhaila and J. M. F. Moura, "Discrete signal processing on graphs," *IEEE. Trans. Signal Process.*, vol. 61, no. 7, pp. 1644–1656, Apr. 2013.

[3] A. Sandryhaila and J. M. F. Moura, "Discrete signal processing on graphs: Frequency analysis," *IEEE. Trans. Signal Process.*, vol. 62, no. 12, pp. 3042–3054, Jun. 2014.

[4] D. I. Shuman, S. K. Narang, P. Frossard, A. Ortega, and P. Vandergheynst, "The emerging field of signal processing on graphs: Extending high-dimensional data analysis to networks and other irregular domains," *IEEE Signal Process. Mag.*, vol. 30, no. 3, pp. 83–98, May 2013.

[5] I. Jestrović, J. L. Coyle, and E. Sejdić, "Differences in brain networks during consecutive swallows detected using an optimized vertex-frequency algorithm," *Neuroscience*, vol. 344, pp. 113–123, 2017.

[6] L. Stanković, M. Daković, and T. Thayaparan, *Time-Frequency Signal Analysis with Applications*, Norwood, MA, USA: Artech House, Mar. 2013.

[7] N. E. Huang *et al.*, "The empirical mode decomposition and the Hilbert spectrum for nonlinear and non-stationary time series analysis," *Proc. Roy. Soc. London A, Math., Phys. Eng. Sci.*, vol. 454, no. 1971, 1998.

[8] L. Cohen, *Time-frequency Analysis*. Upper Saddle River, NJ, USA: Prentice-Hall, 1995.

[9] B. Boashash, ed, *Time-Frequency Signal Analysis and Processing, A Comprehensive Reference*, New York, NY, USA: Academic, 2015.

[10] L. Stanković, "A measure of some time–frequency distributions concentration," *Signal Process.*, vol. 81, no. 3, pp. 621–631, Mar. 2001.

[11] D. I. Shuman, B. Ricaud, and P. Vandergheynst, "Vertex-frequency analysis on graphs," *Appl. Comput. Harmon. Anal.*, vol. 40, no. 2, pp. 260–291, Mar. 2016.

[12] H. Behjat, U. Richter, D. Van De Ville, and L. Sornmo, "Signal-adapted tight frames on graphs," *IEEE Trans. Signal Process.*, vol. 64, no. 22, pp. 6017–6029, Nov. 2016.

[13] D. Hammond, P. Vandergheynst, and R. Gribonval, "Wavelets on graphs via spectral graph theory," *Appl. Comput. Harmon. Anal.*, vol. 30, no. 2, pp. 129–150, 2011.

[14] A. Sakiyama and Y. Tanaka, "Oversampled graph Laplacian matrix for graph filter banks," *IEEE Trans. Signal Process.*, vol. 62, no. 24, pp. 6425–6437, Dec. 2014.

[15] I. Jestrović, J. L. Coyle, and E. Sejdić, "A fast algorithm for vertex-frequency representations of signals on graphs," *Signal Process.*, vol. 131, pp. 483–491, Feb. 2017.

[16] B. Girault, "Stationary graph signals using an isometric graph translation," in *Proc. Eur. Signal Process. Conf.*, 2015, pp. 1516–1520.

[17] A. G. Marques, S. Segarra, G. Leus, and A. Ribeiro, "Stationary graph processes and spectral estimation," *IEEE Trans. Signal Process.*, vol. 65, no. 22, pp. 5911–5926, Nov. 2017, doi: 10.1109/TSP.2017.2739099.

[18] S. Sardellitti, S. Barbarossa, and P. Di Lorenzo, "On the graph Fourier transform for directed graphs," *IEEE J. Sel. Topics Signal Process.*, vol. 11, no. 6, pp. 796–811, Sep. 2017.

[19] J. A. Deri and J. M. Moura, "Spectral projector-based graph Fourier transforms," *IEEE J. Sel. Topics Signal Process.*, vol. 11, no. 6, pp. 785–795, Sep. 2017.

[20] R. Shafipour, A. Khodabakhsh, G. Mateos, and E. Nikolova, "A digraph Fourier transform with spread frequency components," arXiv:1705.10821

[21] L. Stanković, M. Daković, and E. Sejdić, "Vertex-frequency analysis: A way to localize graph spectral components," *IEEE Signal Process. Mag.*, vol. 34, no. 4, pp. 176–182, Jul. 2017.

[22] M. Tsitsvero, S. Barbarossa, and P. Di Lorenzo, "Signals on graphs: Uncertainty principle and sampling," *IEEE Trans. Signal Process.*, vol. 64, no. 18, pp. 4845–4860, Sep. 2016.

[23] A. Agaskar and Y. M. Lu, "A spectral graph uncertainty principle," *IEEE Trans. Inf. Theory*, vol. 59, no. 7, pp. 4338–4356, Jul. 2013.

[24] L. Stanković, M. Daković, and E. Sejdić, "Vertex-frequency energy distributions," *IEEE Signal Process. Lett.*, vol. 25, no. 3, pp. 358–362, Mar. 2018.

GENERAL INSTRUCTION

- **Authors: We cannot accept new source files as corrections for your paper. If possible, please annotate the PDF proof we have sent you with your corrections and upload it via the Author Gateway. Alternatively, you may send us your corrections in list format. You may also upload revised graphics via the Author Gateway.**

QUERIES

Q1. Author: Please confirm or add details for any funding or financial support for the research of this article.
Q2. Author: Please check if the postal code in the affiliation for the author E. Sejdić is okay as set.
Q3. Author: Please provide the full form of acronym GDFT and define it on its first occurrence.
Q4. Author: Please provide the book's author's name for Ref. [9].
Q5. Author: Please update Ref. [20].